Corrosion Electrochemical Behaviors of Titanium in HCl-acidizing Fluid Used in Natural Gas Exploitation

Xiankang Zhong[1,], Siyu Yu[1], Junying Hu[1], Longjun Chen[1], Yufan Shi[2], Zhi Zhang[1], Shujun Gao[3], Dezhi Zeng[1], Taihe Shi[1]*

[1] State Key Laboratory of Oil and Gas Reservoir Geology and Exploitation, School of Oil and Natural Gas Engineering, Southwest Petroleum University, Chengdu 610500, China
[2] School of Applied Technology, Southwest Petroleum University, Nanchong 637001, China
[3] Department of Chemical & Biomolecular Engineering, Ohio University, OH 45701, United States
[*]E-mail: zhongxk@yeah.net

The corrosion electrochemical behaviors of titanium in HCl-acidizing fluid used in natural gas exploitation were investigated using weight loss measurement, polarization curves and electrochemical impedance spectroscopy. The surface morphologies and composition of sample before and after corrosion were examined using electron scanning microscope coupled with energy dispersive spectrometer. The results show that corrosion resistance of titanium in HCl-acidizing fluid depends on the balance between the dissolution and formation of passive film on titanium. This balance shifts towards the dissolution as the HCl content increases, causing a decrease in corrosion resistance. The remaining dissolved-oxygen in the solution accelerates the formation of passive film and therefore the corrosion resistance first increases with time, then, the formation of passive film is delayed because of depletion of dissolved-oxygen, hence a decrease in corrosion resistance.

1. INTRODUCTION

The search for hydrocarbon reserves continues to go to the deeper formation where completions have requirements for high tensile loading, high pressure and high temperature. These wells are commonly referred to as high pressure, high temperature (HPHT) wells [1]. HTHP wells usually have to contend with H_2S, CO_2, and chlorides at high temperatures. In this case, corrosion resistant alloys such as nickel-base alloys are required to be selected for downhole tubulars and components. However, corrosion resistant alloys can be very expensive particularly considering that some HPHT wells are being considered for completion depths well of over 30000 feet (more than 9000

meters) [2]. Titanium alloys can potentially be for an alternative to conventional corrosion resistant alloys due to their combinations of high strength, low density and high corrosion resistance. Although the price for titanium alloys has historically been higher than that for corrosion resistant alloys (e.g. nickel-base alloys), titanium alloys are approximately half as dense as nickel-base alloys so titanium alloy can provide twice the length of tubing per unit of weight. With the development of the metallurgical and manufacturing techniques, the price for titanium alloys is expected to decrease further, resulting in that titanium alloys are more competitive as downhole tubulars and components materials.

Titanium is a reactive metal. However, the corrosion resistance of titanium and its alloys originates from the formation of a tenacious, thin and protective oxide surface film which makes titanium and its alloys versatile for many applications, such as aeronautics [3], medical implant materials [4-7], and nuclear reprocessing plant [8, 9]. Titanium alloys have also been successfully applied in oil and gas field [10]. For example, a specific titanium alloy called Ti 6246 (UNS R56260) has been used by Chevron for more than 20 years in downhole service as logging tools [2]. It is recently reported that titanium alloy (the exact composition is not published) tubing jointly developed by Sinopec Corp and Tianjin Iron and Steel Group has been applied since 2015 in Yuanba gas well located in Langzhong, Sichuan, China [11]. The titanium alloy tubing reached a depth of 6448 meters. It is claimed that this is the first successful experience of titanium alloy petroleum special pipes putting into practice in the super-deep gas well with high content of H_2S across the world.

Extensive work in laboratory has been conducted on the corrosion assessment of titanium alloys exposed to several simulated downhole environments including sour production environments, packer fluids, stimulation acids, and methanol [1, 2, 12-16]. The data from these corrosion assessments show that titanium alloys are highly resistant to H_2S, CO_2 and brine under a wide range of conditions. However, titanium alloys are extremely susceptible to severe corrosion in typical acidizing fluids such as HCl and HF. Chambers and co-authors [12] reported that Ti 64 (UNS R56400) and Ti 6246 (UNS R56260) coupons were all completely dissolved during the 8 h of exposure in 10 wt.% HCl solution with 0.1 MPa H_2S at 232 ^{o}C, translating to minimum corrosion rates in the range of 406 mm/y to 1049 mm/y. Klink and co-authors [13] found that severe corrosion degradation for Ti-3Al-8V-6Cr-4Zr-4Mo alloy in 15 wt.% HCl solution, and in 12 wt.% HCl mixed with 3 wt.% HF solution could occur. The corrosion rate for this titanium alloy in the former solution and the latter one is over 519 mm/y and 741 mm/y, respectively.

The use of acidizing fluids is a common practice in oil and gas production where acids are pumped through tubular goods into an oil or gas reservoir in order to remove formation damage, increase porosity in the formation, and clean deposits from tubulars. The essential in nature of corrosion of titanium alloys in acidizing fluids is one or more electrochemical reactions which occurs at the alloy/solution interface. Unfortunately, owing to the some limitations and difficulties for electrochemical test in the simulated downhole environments (i.e. high temperature, high pressure and high content of H_2S), almost all of the tests in current literatures were conducted only using the weight loss measurement. Although the corrosion behaviors of titanium and its alloys have been substantially investigated [17-21], the corrosion mechanisms of titanium in HCl-acidizing acid solution used in natural gas exploitation are still missing. Electrochemical techniques are the very important tools to

understand the corrosion mechanisms of metal materials, which have been widely used in corrosion mechanisms analysis of alloys used in environment containing CO_2, or H_2S or Cl^- [22-29]. Therefore, the study on corrosion behaviors of titanium and titanium alloys using electrochemical techniques in acidizing fluids are highly significant for understanding the corrosion mechanisms.

Although it is well known that commercial grade titanium should not be used in highly concentrated HCl, the pure titanium in HCl-acidizing fluid was still used in this work for more depth of understanding in corrosion electrochemical mechanism. In the present work, the corrosion behaviors of pure titanium in HCl-acidizing fluid were studied using polarization curves, electrochemical impedance spectroscopy, as well as weight loss measurement. Moreover, the surface morphologies and the composition of sample before and after corrosion were examined by using scanning electronic microscope coupled with energy dispersive spectrometer.

2. EXPERIMENTAL

2.1. Sample and solution

Samples which were cut from a commercial pure titanium pipe (ZS Advanced Material Co., Ltd., China) were used in this work. All the samples were evenly polished by sand paper with 600 and 800 grit numbers, sequentially, and then cleaned in an ultrasonic bath with petroleum ether. Samples then were taken out and dried by nitrogen gas and immediately used for measurement. The 1 wt.% NaCl solution with different HCl contents (5, 10 and 18 wt.%) was prepared from deionized water (18.2 MΩ cm in resistivity) and analytical grade reagents. The test solution was deoxygenated with a continuous N_2 gas flow purge. All the experiments were carried out at 40 $^{\circ}$C and atmospheric pressure.

2.2. Weight loss measurement

The sample with dimensions of 40 mm×10 mm × 7 mm was used in weight loss measurements. After 72 h of immersion, the average corrosion rate was calculated by equation (1):

$$v = 87600 \frac{\Delta m}{\rho A \Delta t} \qquad (1)$$

where v is the corrosion rate (mm/y), Δm is the weight loss (g) before and after immersion, ρ is the density of pure titanium (g/cm^3), A is the sample surface area (cm^2) and Δt (h) is the immersion time.

2.3. Electrochemical tests

The electrochemical tests, including polarization curves and electrochemistry impedance spectroscopy (EIS), were conducted using a CS 350 electrochemical workstation (Wuhan Corrtest Instruments Corp. Ltd., China). A conventional three-electrode configuration was employed in the tests where a saturated calomel electrode (SCE) was used as a reference electrode and Pt sheet was

used as a counter electrode. A cylindrical titanium sample used as working electrode was embedded in an epoxy cylinder where the exposed surface area is 0.4 cm^2. Polarization curves were performed by shifting the potential from -0.5 V (vs. Opening Circuit Potential, OCP) to +4.5 V (vs. OCP) with a scanning rate of 0.5 mV/s. The EIS measurements were performed at OCP with a peak-to-peak 5 mV sinusoidal perturbation at the frequency from 10000 Hz to 10 mHz, with 12 points per decade. Z-view software was used to analyze the EIS data. In order to check the reproducibility, all the electrochemical measurements were repeated at least three times.

2.4. Characterization of surface morphologies and composition

The surface morphologies of samples were observed by digital camera and scanning electronic microscopy (SEM, Phillips Quanta 200, America) and the surface composition was also detected by energy dispersive spectroscopy.

3. RESULTS

3.1. Weight loss

The average corrosion rates of titanium after 72 h of immersion in deoxygenated 1 wt.% NaCl solution containing different contents of HCl at 40 ^{o}C are shown in Figure 1. It is seen that the corrosion rate of titanium increases with increasing HCl content. As an increase in HCl content from 5 wt.% to 10 wt.% and 18 wt.%, the corrosion rate increases from 0.64 mm/y to 1.09 mm/y and 2.92 mm/y.
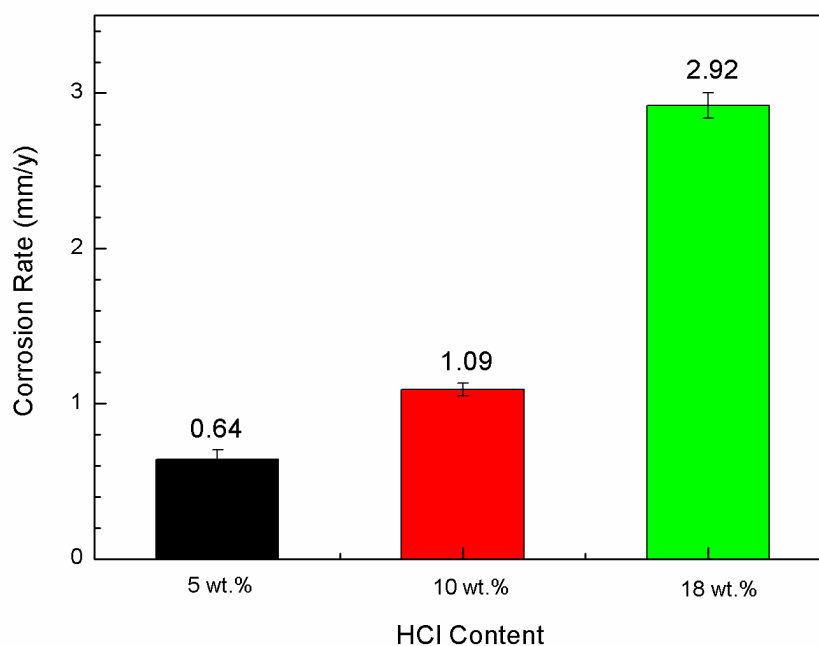
Figure 1. The average corrosion rates of titanium after 72 h of immersion in deoxygenated 1 wt.% NaCl solution containing different contents of HCl at 40 ^{o}C. The error bars on the figure indicate standard deviation.

3.2. Polarization curves

Figure 2 shows typical polarization curves for titanium in deoxygenated 1 wt.% NaCl solution with different contents of HCl at 40 °C. It can be seen that the linear Tafel region for every anodic side is essentially nonexistent, but it is obviously present at each cathodic side. Therefore, the corrosion potential (E_{corr}) and corrosion current density (i_{corr}) in this work were obtained by Tafel extrapolation of the cathodic site. The related parameters are listed in Table 1. Subsequently, the corrosion rates (*v*, mm/y) can be calculated according to equation (2):

$$v = 87600 \frac{M i_{corr}}{nF\rho} \qquad (2)$$

where *M* is the molar mass (g/mol) of titanium, ρ is the density of pure titanium (g/cm^3), *F* represents Faraday constant (*F*=26.8 A•h) and *n* is the number of electrons involved in the dissolution of titanium (*n*=2). As is shown in Table 1, the E_{corr} slightly decreases with increasing HCl content, and simultaneously the i_{corr} rapidly increases with increasing HCl content. Accordingly, the corrosion rate increases from 0.84 mm/y in 5 wt.% HCl solution to 1.47 mm/y in 10 wt.% HCl. And the corrosion rate for titanium in 18 wt.% HCl solution is about four times larger than that in 5 wt.% HCl solution. Note that this corrosion rate is a transient corrosion rate after 1 h of immersion and the corrosion rate obtained from the weight loss measurement is an average corrosion rate during the 72 h of immersion. A difference in corrosion rate between weight loss measurement and Tafel extrapolation calculation is therefore present.
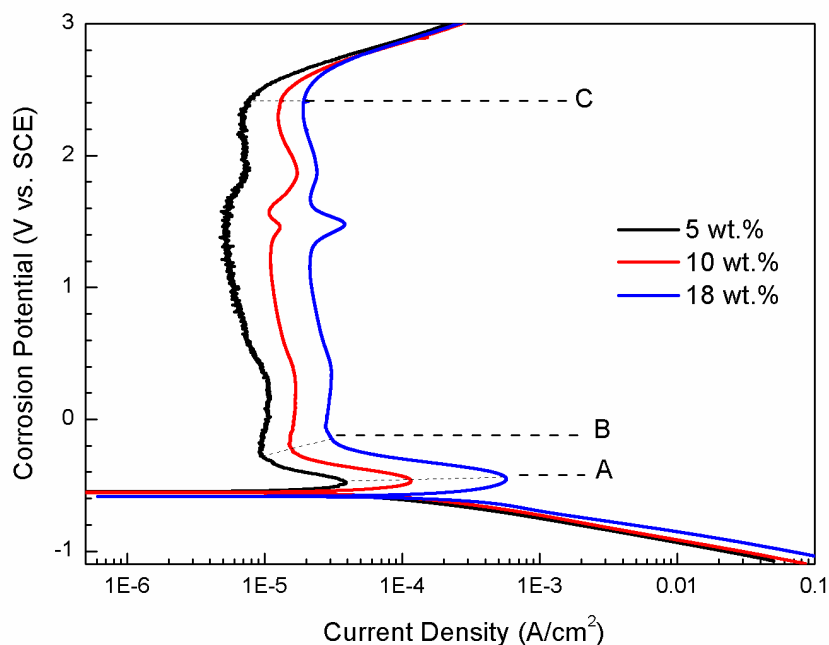
Figure 2. Typical polarization curves of titanium in deoxygenated 1 wt.% NaCl solution containing different contents of HCl at 40 °C.

As is shown in Figure 2, typical passivity characteristics can be found from the anodic polarization curves. Beginning with the open circuit potential and moving in the anodic direction, it

firstly passes through a region of active corrosion in which current density with respect to the titanium dissolution increases with increasing potential. Then, the current density reaches a maximum value (point A shown in Figure 2) and subsequently decreases abruptly. The potential at point A is referred to as the critical (primary) passivation potential (E_{cp}). As listed in Table 1, it can be found that E_{cp} increases with increasing HCl content from -0.478 V vs. SCE in 5 wt.% HCl solution to -0.462 V vs. SCE in 10 wt.% HCl solution and -0.448 V vs. SCE in 18 wt.% HCl solution. Another important parameter of the passivation process is the critical passivation current density (i_{cc}) which is required to attain the E_{cp}. It can be seen from Table 1 that i_{cc} largely increases with increasing HCl content. E.g., i_{cc} of titanium in 18 wt.% HCl solution is about 14 times larger than that in 5 wt.% HCl.

Table 1. The electrochemical parameters obtained from the polarization curves of titanium in deoxygenated 1 wt.% NaCl solution containing different contents of HCl at 40 ^{o}C.

HCl content (wt.%)	E_{corr} (V vs. SCE)	i_{corr} (A/cm^2)	E_{cp} (V vs. SCE)	v_{corr} (mm/a)	i_{cc} (A/cm^2)	E_F (V vs. SCE)	i_p (A/cm^2)	E_o (V vs. SCE)
5	-0.550	4.84e-5	-0.480	0.84	3.86e-5	-0.276	9.26e-6	2.330
10	-0.555	8.47e-5	-0.462	1.47	1.15e-4	-0.200	1.51e-5	2.330
18	-0.584	1.96e-4	-0.448	3.41	5.68e-4	-0.058	2.66e-5	2.338

A further increase in potential above point A causes a decrease in the anodic current density. This is because a passive film is being formed on the titanium surface. When the titanium surface is completely covered with a passivating film, the anodic current density becomes independent of potential. The most negative potential at which this state is attained is called the Flade potential (E_F) [30], as is shown as point B in the Figure 2. It should be pointed out that some researchers also called critical passive potential as Flade potential [31]. Flade potential here represents the most negative limit of stability of the passive state. As shown in Table 1, E_F of titanium in 5 wt.% HCl, 10 wt.% HCl and 18 wt.% HCl is -0.276 vs. SCE, -0.200 vs. SCE and -0.058 V vs. SCE, respectively, showing a significant increase in E_F with increasing HCl content. The current density at the passive state can be called as the passive current density (i_p). The i_p at point B (at E_F of each sample, respectively) listed in Table 1. It shows that i_p strongly depends on HCl content and a sharply increase in i_p with increasing HCl content can be seen. The passive state of titanium in HCl solution can be maintained at a very wide potential range which exceeds 2.3 V. It should be pointed out that some small peaks around 1.5V vs. SCE can be seen in the passive region from the Figure 2. This is due to chlorine evolution with intensity depending on the electronic properties of the passive film [32].

The region beyond the passive region in which the current density again increases rapidly with increasing potential may be due to the oxygen evolution because the potential (E_o) for each condition are almost the same, as shown in Table 1. Pure titanium would not be expected to suffer pitting corrosion in the given conditions. Therefore, the breakdown of the passive film is not considered here.

3.3. Electrochemistry impedance spectroscopy
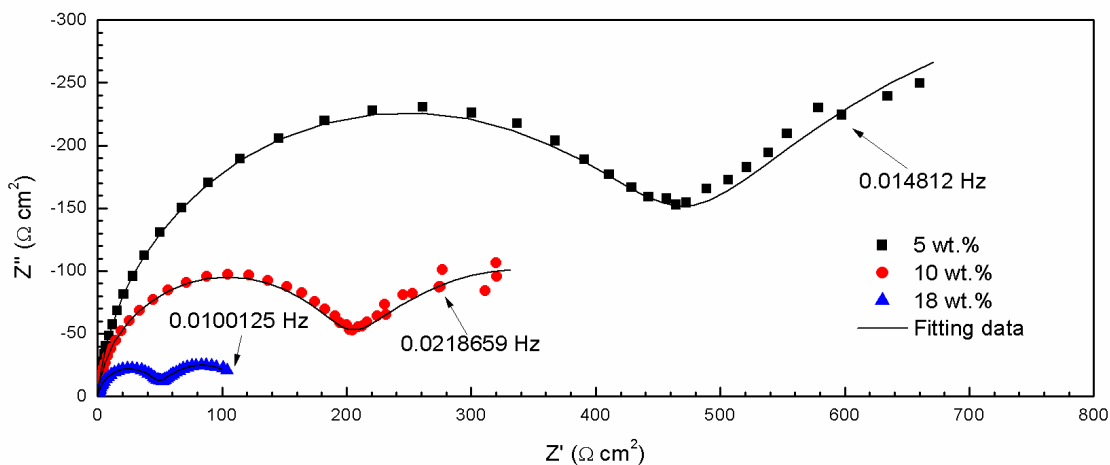
Figure 3. Nyquist plots of EIS data of titanium after 1 h of immersion in deoxygenated 1 wt.% NaCl solution containing different contents of HCl at 40 $^{\circ}$C.
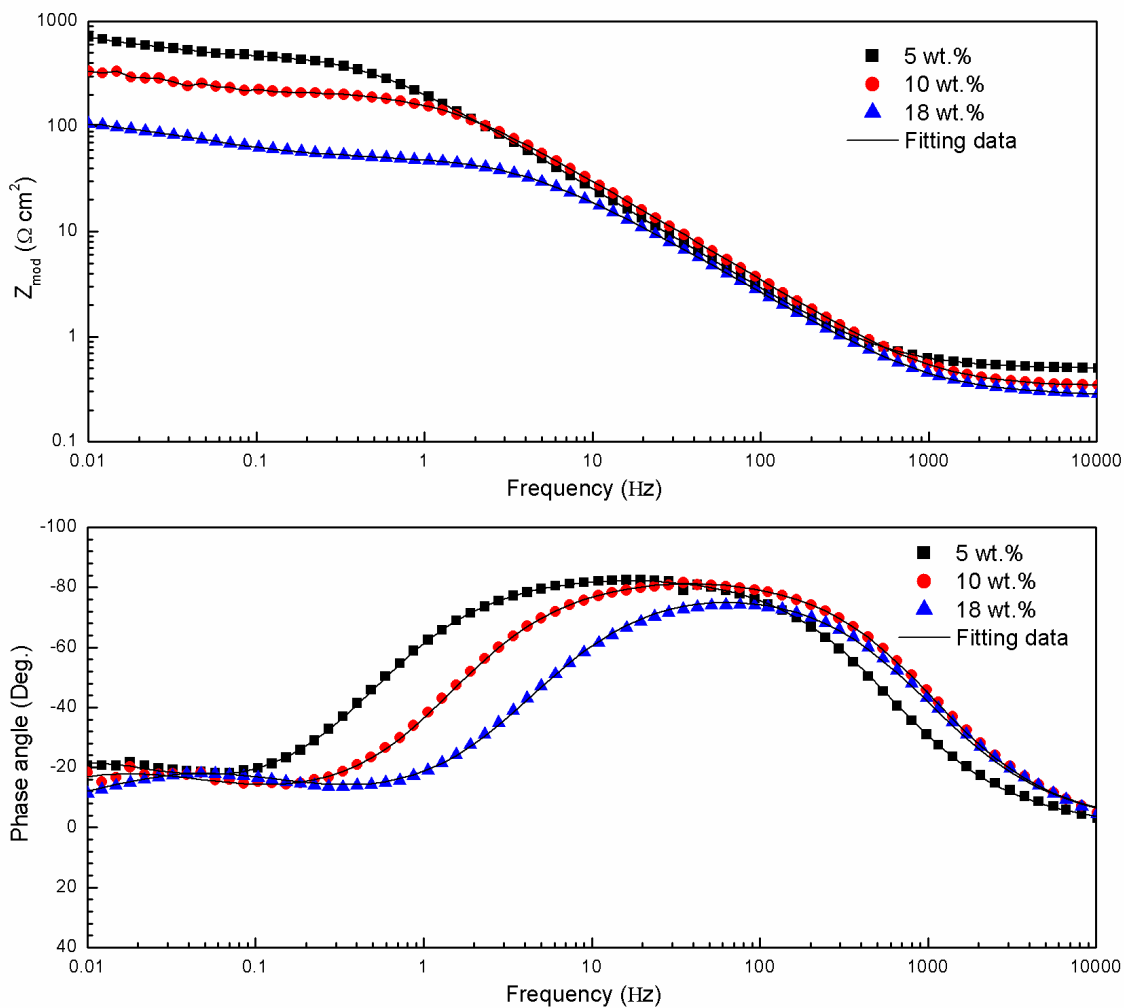
Figure 4. Bode plots of EIS data of titanium after 1 h of immersion in deoxygenated 1 wt.% NaCl solution containing different contents of HCl at 40 $^{\circ}$C.
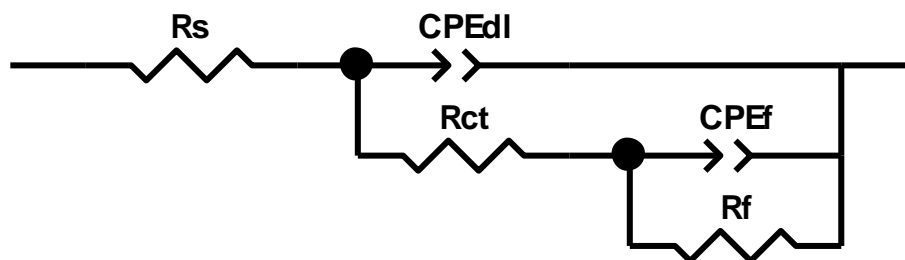
Figure 5. The equivalent circuit used for the EIS data fitting in this work. R_s represents solution resistance between work electrode and reference electrode, R_{ct} represents charge transfer resistance and R_f refers the resistance of passive film formed on the titanium electrode surface. CPE_{dl} and CPE_f represent the double layer capacitance and the capacitance of passive film on the electrode surface, respectively.

The EIS data of titanium in deoxygenated 1 wt.% NaCl solution containing different contents of HCl after 1 hour of immersion at 40 ^{o}C are shown in Figures 3 and 4. It is seen from Figure 3 that all the Nyquist plots exhibit two capacitive semicircles. The diameters of semicircles (includes the semicircles on the left and right) sharply decrease with increasing content of HCl. In Bode plots shown in Figure 4, the modulus of impedance (Z_{mod}) decreases as the HCl content increases, and simultaneously the maximum phase angles shift towards right (lower frequency region) and decrease from about -80° to approximately -74° as the HCl content increases from 5 wt.% to 18 wt.%.

In order to analyze the corrosion electrochemical mechanism, an equivalent circuit was proposed to fit the EIS data, as is show in Figure 5, where R_s represents solution resistance between work electrode and reference electrode, R_{ct} represents charge transfer resistance and R_f refers the resistance of passive film formed on the titanium electrode surface. The constant phase element (CPE) was employed in the equivalent circuit instead of the ideal capacitance. The impedance of CPE is given by equation (3):

$$Z_{CPE} = [C(j\omega)^n]^{-1} \qquad (3)$$

where C is the capacitance of an ideal capacitor, $j\omega$ is the complex variable for sinusoidal perturbations which $\omega=2\pi f$, and the exponent n ($-1 \le n \le 1$) is associated with non-uniform distribution of current as a result of roughness and surface defects. CPE_{dl} and CPE_f represent the double layer capacitance and the capacitance of passive film on the electrode surface, respectively. As is shown for the solid line in Figures 3 and 4, this equivalent circuit fits the EIS data well. Another equivalent circuit model which is usually called two-layer oxide model composed of a porous outer layer and a dense inner layer has been commonly used in some studies on titanium or titanium alloys in relatively moderate corrosive media such as Hank's solution, NaCl solution and artificial siliva [5, 33, 34]. It is reasonable if that inner layer is dense enough to hinder the penetration of the electrolyte to the metal substrate. However, in the present work high contents of HCl solutions were used and the whole oxide layer might not be dense enough or even incomplete, so that titanium may be contact directly with the corrosive ions. Therefore, an equivalent circuit with respect to the passive film and the reaction occurred at titanium/solution interface shown in Figure 5 was used in the present work. Similar equivalents circuit fitting model was also proposed by Wang and co-authors who studied the titanium alloys in H$_2$SO$_4$ with a high concentration [23]. The values of R_s, CPE_{dl}, R_{ct}, CPE_f and R_f derived from

fitting are listed in Table 2. It can be seen that the R_{ct} and R_f decrease with increasing HCl content. E.g., R_{ct} of the titanium electrode decreases from 476 Ω cm^2 in 5 wt.% HCl solution to 201 Ω cm^2 in 10 wt.% HCl solution and about 49 Ω cm^2 in 18 wt.% HCl solution (See Table 2).
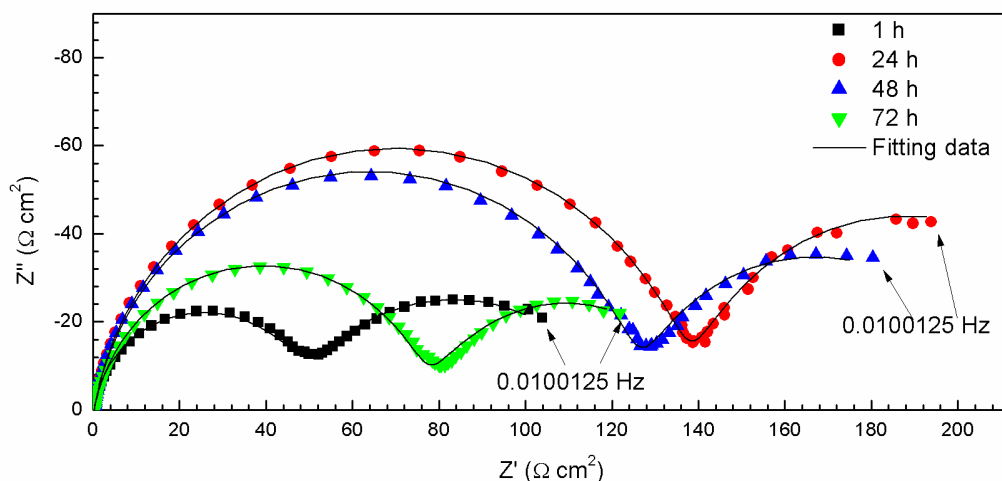
Figure 6. Nyquist plots of EIS data of titanium after different immersion time in deoxygenated 1 wt.% NaCl solution containing 18 wt.% HCl at 40 ^{o}C.
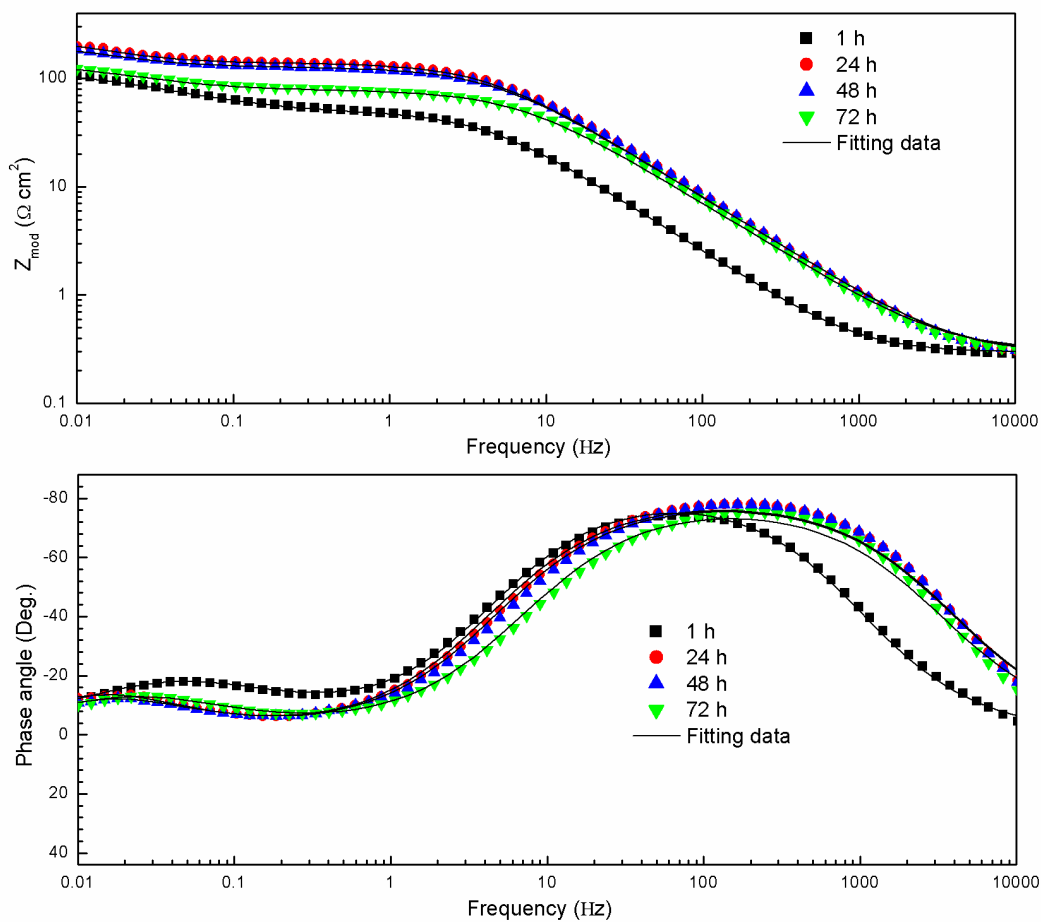
Figure7. Bode plots of EIS data of titanium after different immersion time in deoxygenated 1 wt.% NaCl solution containing 18 wt.% HCl at 40 ^{o}C.

Table 2. Fitting parameters of EIS of titanium in deoxygenated 1 wt.% solution containing different contents of HCl at 40 °C.

HCl content (wt.%)	R_s (Ω cm^2)	CPE_{dl} (F cm^{-2} Hz$^{1-n_1}$)	n_1	R_{ct} (Ω cm^2)	CPE_f (F cm^{-2} Hz$^{1-n_2}$)	n_2	R_f (Ω cm^2)
5	0.51	7.53e-4	0.95	476.4	2.19e-2	0.79	807.8
10	0.35	6.31e-4	0.95	201.3	3.09e-2	0.75	289.1
18	0.30	9.88e-4	0.93	48.6	5.79e-2	0.75	72.3

Figures 6 and 7 show the EIS data of titanium in deoxygenated 1 wt.% NaCl solution containing 18 wt.% HCl with different immersion time. It can be seen that the diameter of the capacitance semicircle first increases and then decreases with time. And the corresponding parameters fitted by the equivalent circuit (Shown in Figure 5) are also listed in Table 3. According to the fitting results, both R_{ct} and R_f first increase and then decrease with time, and the maximum values of R_{ct} and R_f are present at 24 h of immersion.

Table 3. Fitting parameters of EIS of titanium in deoxygenated 1 wt.% solution containing 18 wt.% HCl after different immersion time at 40 °C.

Time (h)	R_s (Ω cm^2)	CPE_{dl} (F cm^{-2} Hz$^{1-n_1}$)	n_1	R_{ct} (Ω cm^2)	CPE_f (F cm^{-2} Hz$^{1-n_2}$)	n_2	R_f (Ω cm^2)
1	0.30	9.88e-4	0.93	48.6	0.06	0.75	72.3
24	0.29	3.76e-4	0.90	139.0	0.11	0.90	100.6
48	0.30	3.82e-4	0.90	127.0	0.11	0.88	82.0
72	0.31	4.54e-4	0.89	77.6	0.01	0.80	65.0

3.4. Surface morphology and composition

Figure 8 shows optical graphs of the freshly polished titanium sample and the samples after 72 h of immersion in deoxygenated 1 wt.% NaCl solution containing various contents of HCl at 40 °C. As compared with the freshly polished sample, the surface of the samples after 72 h of immersion in HCl containing solution becomes rough and the metal luster has totally disappeared. In order to get more micro-level information of the surface morphology, Figure 9 shows the SEM images of the freshly polished titanium sample, and the images of titanium after 72 h of immersion in deoxygenated 1 wt.% NaCl solution containing various contents of HCl at 40 °C. Figure 9a shows the initial surface state of the polished titanium sample. Some fine scratches resulting from the polishing process are visible in the image. After 72 h of immersion, the initial scratches on the sample in HCl-containing solutions (See Figures 9b, c and d) cannot be found any more. Instead, honeycomb surface morphologies are present. As the HCl content increases, the honeycomb holes with bigger diameter and greater depth can be found on the sample surface. The surface composition of titanium in deoxygenated 1 wt.% NaCl solution containing 18 wt.% HCl for 72 h at 40 °C is also shown in Figure 10. Ti and C elements

were detected from the corroded surface, however, O element did not be found, this is because the passive film on titanium is too thin to be detected by energy dispersive spectrometer.
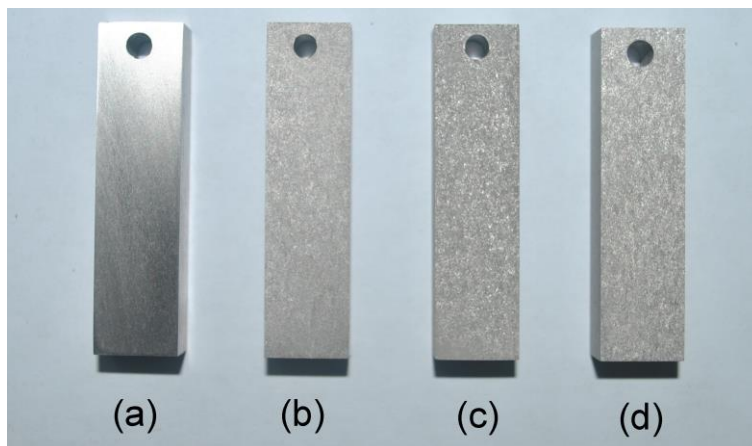
Figure 8. Optical graphs of (a) titanium sample surface after being polished, and titanium after 72 h of immersion in deoxygenated 1 wt.% NaCl solution containing various contents of HCl (b) 5 wt.%, (c) 10 wt.% and (d) 18 wt.% at 40 ^{o}C.
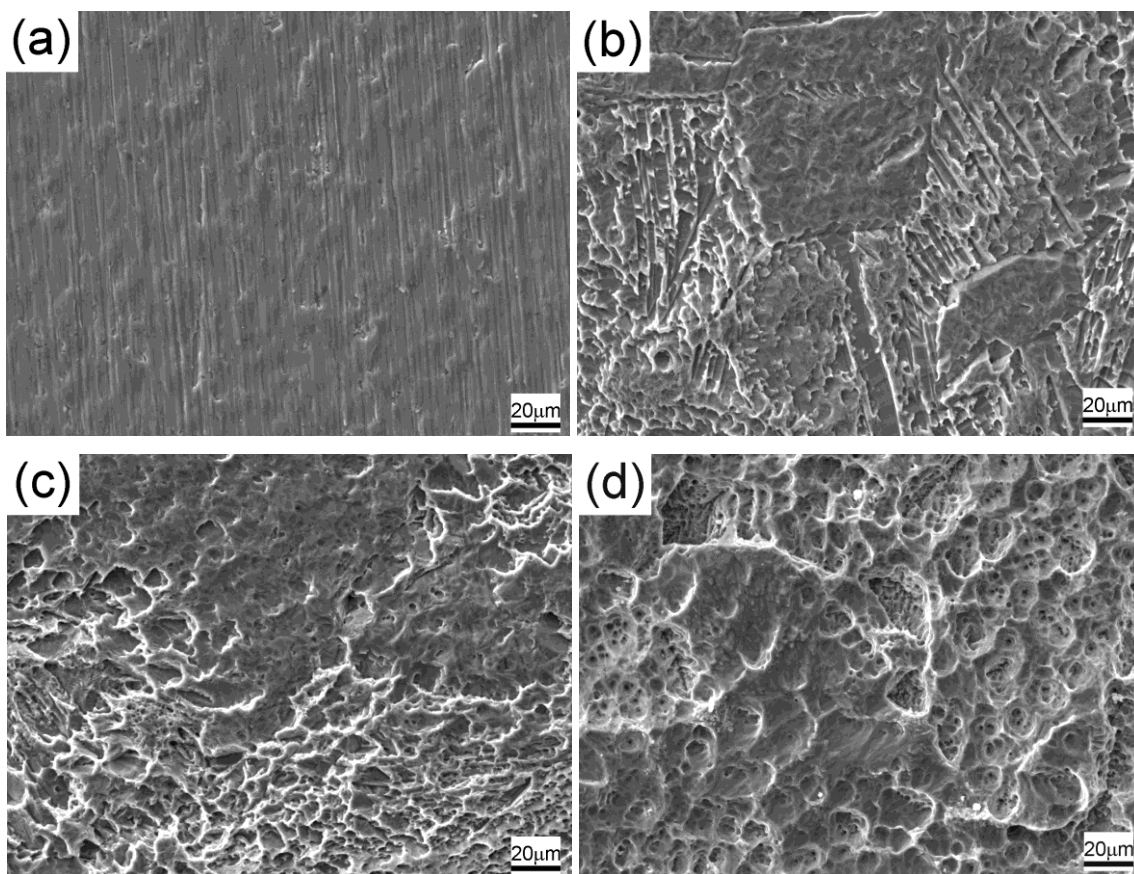
Figure 9. SEM images of (a) titanium sample surface after being polished, and titanium after 72 h of immersion in deoxygenated 1 wt.% NaCl solution containing various contents of HCl (b) 5 wt.%, (c) 10 wt.% and (d) 18 wt.% at 40 ^{o}C.
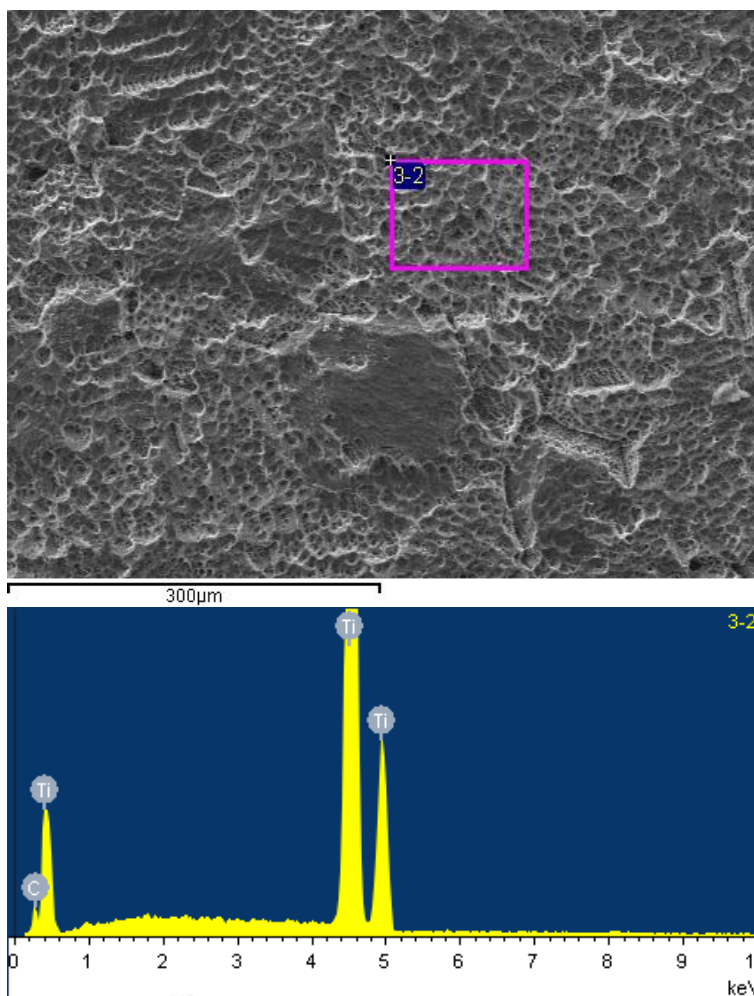
Figure 10. EDS of titanium after 72 h of immersion in deaearated 1 wt.% NaCl solution containing 18 wt.% HCl at 40 °C.

4. DISCUSSION

4.1. The corrosion of titanium in HCl-acidizing fluid

In actual fact titanium is particularly stable in the presence of the majority of non-fluorinated aqueous solutions. It was also reported that if the solution is moderately oxidizing, titanium can be considered to be safe from corrosion [35]. However, in this work the deoxygenated HCl-acidizing fluid is not oxidizing, combined with the high activity of titanium, server corrosion for titanium is therefore expected to occur. The main anodic reactions are as follows:

$$Ti \rightarrow Ti^{2+} + 2e^- \qquad (4)$$
$$Ti^{2+} \rightarrow Ti^{3+} + e^- \qquad (5)$$

According to the Pourbaix (potential vs. pH) diagram of titanium in water at 25 °C , the domain of predominance of Ti^{2+} lies entirely below the line corresponding to the equilibrium of the reaction of the reduction of water to gaseous hydrogen at atmospheric pressure [35]. This ion is therefore unstable and tends to be oxidized to Ti^{3+} which is stable in a solution with a very low pH. The presence of Ti^{3+} in the solution can also be confirmed by the solution color changes in the weight loss measurement in

this work. The color of the solution changed from the colorless at the very beginning to violet at the later stage of immersion. A similar phenomenon were also reported in reference [23], where an obvious variation from colorless to violet in color of the solution during the immersion tests. This was attributed to the presence of Ti^{3+} in the solution. The dominant cathodic reaction in this work should be the reduction of H^+:

$$2H^+ + 2e^- \rightarrow H_2 \qquad\qquad (6)$$

however, it is necessary to mention that the reduction of the remaining dissolved-oxygen in the solution should also be involved in the cathodic reaction of titanium in HCl-acidizing fluid:

$$4H^+ + O_2 + 4e^- \rightarrow 2H_2O \qquad\qquad (7)$$

The corrosion rate of titanium in HCl-acidizing fluid strongly depends on the passive film which may be originally formed before titanium was exposed to the solution or be formed during the immersion. The passive oxide film could be formed during the polishing and cleaning processes where massive oxygen and water create a favorable environment for the formation of passive film. On the other hand, the remaining dissolved-oxygen in deoxygenated HCl solution may also result in the formation of a passive film on titanium. The polarization curves (Figure 2) show that the passive film can be easily formed on titanium surface under certain ranges of anodic polarization in deoxygenated HCl solution, resulting in a very low passive current density (Table 1), even if the content of HCl increases up to 18 wt.%, the passive current density is still as low as 2.66×10^{-5} A/cm^2. Nakagawa and co-authors reported that an increase in the dissolved oxygen concentration in artificial saliva tended to increase the corrosion resistance of titanium [36]. These demonstrate that a protective passive film could be formed on the titanium by oxidation process. This oxidation can originate from an anodic polarization with certain potentials or an oxidant such as O_2. It is rather complicated for the formation mechanism of passive film on titanium because the complex changes in valence of titanium may occur and consequently different titanium compounds may get involved in the formation process of the passive film. However, it has been well accepted that a stable passive film is composed of TiO_2 which is highly thermodynamically stable in the presence of water or aqueous solution. This TiO_2 film could be highly protective and this is why titanium is particularly stable in the common aqueous solution. Meanwhile, the Pourbaix diagram also shows that if the solution pH is extremely low and in the absence of a certain range of anodic polarization potential on titanium surface, TiO_2 film could be dissolved [35]. Therefore, it can be considered that the corrosion rate of titanium in HCl-acidizing fluid depends on the balance between the formation and dissolution of passive film. This balance will shift as the condition varies. For example, the average corrosion rate during the 72 h of immersion (Figure 1) and the transient corrosion rate at 1 h (Table 1) increase with increasing HCl content, indicating that more serious corrosion for titanium occurs in higher content of HCl solution because the balance shifts more towards the dissolution of passive film on titanium. i.e., the passive film on titanium in the solution with a higher HCl content is destroyed more seriously than that in the solution with a lower HCl content. While, the charge transfer resistance and the resistance of passive film on titanium in 18 wt.% HCl solution first increase and then decrease with time. This can be attributed to that the presence of the remaining dissolved-oxygen in the solution accelerates the formation of passive film, making the balance first moves towards the passive film formation, and as the dissolved-oxygen being depleted, this balance then moves towards the dissolution of passive film. This will be discussed in

detail in Section 4.3.
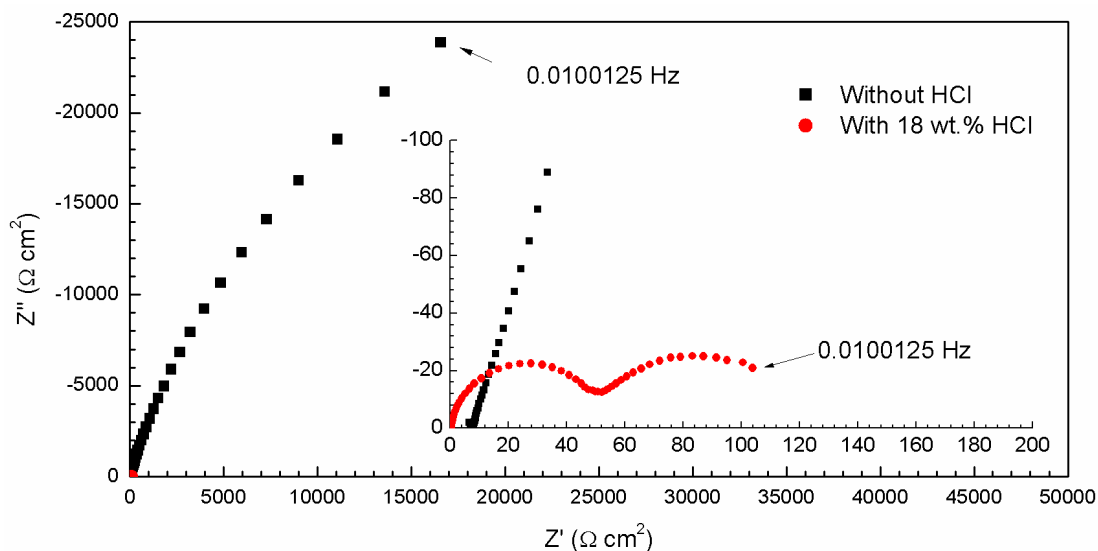
Figure 11. Nyquist plot of EIS data of titanium after 1 h of immersion in deoxygenated 1 wt.% NaCl solution with and without HCl at 40 ^{o}C.
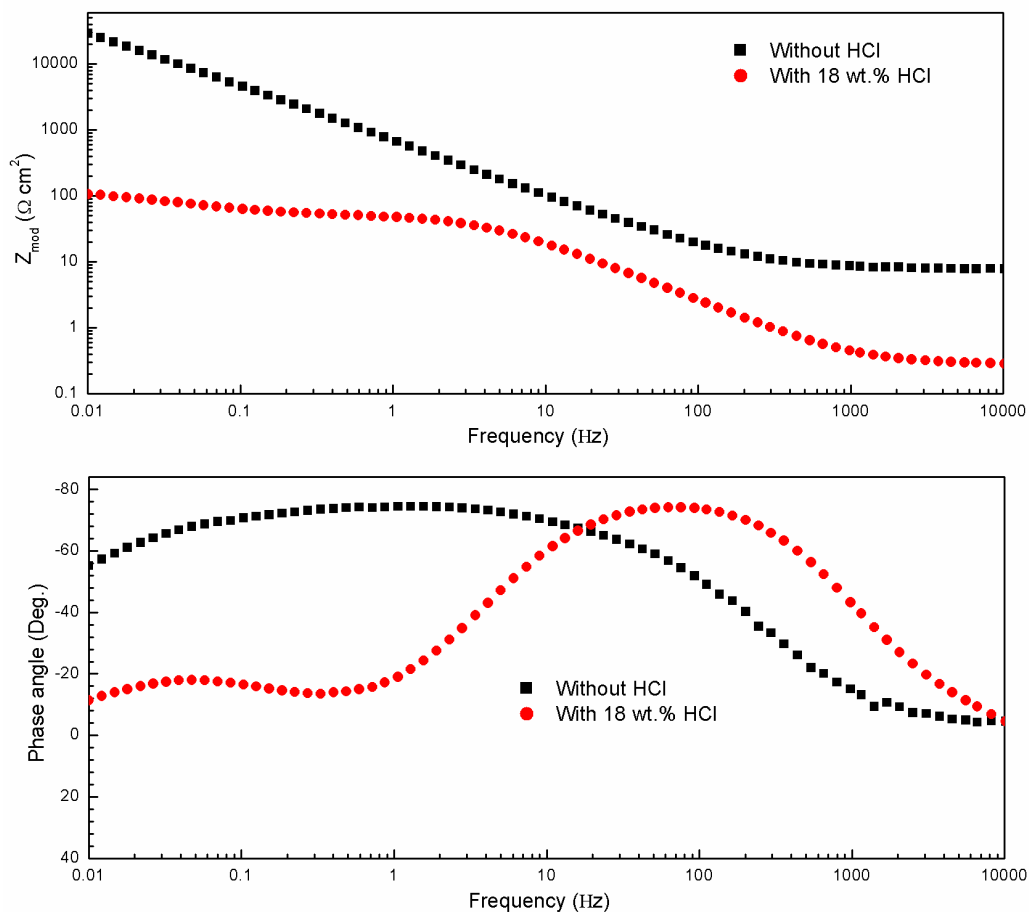
Figure 12. Bode plot of EIS data of titanium after 1 h of immersion in deoxygenated 1 wt.% NaCl solution with and without HCl at 40 ^{o}C.

SEM images of titanium after 72 h of immersion in HCl solutions show honeycomb surface morphologies (Figure 9). Therefore, it could be considered that the passive film on titanium in HCl-acidizing fluid is incomplete. And this assumption can be confirmed by a comparison in EIS of titanium in solutions with and without HCl solution. Figure 11 shows the typical Nyquist plots of titanium after 1 h of immersion in deoxygenated 1 wt.% NaCl solution with and without HCl at 40 ^{o}C. It is apparently that there is a big difference in the characteristics of capacitive loops. In the absence of HCl, only one capacitive semicircle with a very big diameter is present. However, there are two capacitive semicircles with very small diameters are present in the presence of 18 wt.% HCl. Wang and co-authors reported that the appearance of two obvious capacitive semicircles is a sign of the remarkable deterioration in the corrosion resistance of titanium [37]. Similarly, there are also obvious differences in Bode plots between with and without HCl, as shown in Figure 12. In the low and middle frequency ranges, the impedance spectra (modulus vs. frequency) in the solution without HCl displayed at linear slope of about -1, which is the characteristic response of a capacitive behavior of a complete passive film. This is in good agreement with the results reported by Bai and co-authors [5]. Moreover, only one time constant can be found in the phase angle vs. frequency plot. However, in the presence of HCl, the impedance spectrum (modulus vs. frequency) is totally different, i.e., the slope of the line in modulus vs. frequency apparently decreases at the low and middle frequency ranges. Simultaneously, two time constants are present in the phase angle vs. frequency plot. These results indicate that the passive film on the titanium in HCl-acidizing fluid has been partially destroyed at least and the balance which determines the corrosion rate of titanium shifts more towards the dissolution of passive film in the presence of HCl.

4.2. Effect of HCl content

The content of HCl of the commonly used HCl-acidizing fluids is in a wide range [12]. Therefore, it is necessary to discuss the effect of HCl content on the corrosion of titanium. As mentioned in Section 3, both the average corrosion rate during the 72 h of immersion and the transient corrosion rate at 1 h of immersion increase with increasing HCl content. While according to the fitting results of the EIS, the charge transfer resistance and the resistance of passive film decrease as the HCl content increases. Therefore, it means that the balance between the dissolution and formation of passive film shifts towards the former one. This can be attributed to that the dissolution of passive film is accelerated as the HCl content increases. The corrosion resistance of passive film decreases and therefore the dissolution rate of titanium substrate increases as the HCl content increases. There is a good consistency between the results of corrosion rate tests and the surface morphology observation. As the HCl content increases, the honeycomb holes with bigger diameter and greater depth can be found on the sample surface (Figure 9). This phenomenon also confirms that the dissolution rate of titanium increases with increasing HCl content.

4.3. Effect of immersion time

It is interesting that the corrosion resistance of titanium in 18 wt.% HCl solution first increases and then decreases with time, and the maximum value is present at 24 h. Actually, the same tendencies were found in the 5 wt.% and 10 wt.% solution through the long term EIS measurement (Not shown). As the parameters listed in Table 3, the charge transfer resistance and the resistance of passive film increase first and then decrease. Both of the maximum values are present at 24 h. As discussed above, the corrosion resistance of titanium strongly depends on the balance between the dissolution and formation of passive film. Before 24 h, this balance tends to shift to the formation of passive film and the corrosion resistance is therefore increasing. This shift in balance can be attributed to the acceleration in the formation of passive film in the presence of remaining dissolved-oxygen in the solution. In order to confirm this, additional weight loss measurements of titanium in deoxygenated 1 wt.% solutions with 5 wt.% and 18 wt.% HCl for 72 h were conducted in this work. As is shown in Figure 13, the corrosion rate for titanium in deoxygenated solutions is apparently lower than that in deoxygenated solutions. For example, the corrosion rate of titanium in deoxygenated and deoxygenated 5 wt.% HCl solution are 0.64 mm/y and 0.42 mm/y, respectively. It means that corrosion rate dropped by about one-third because of the presence of larger amount of O_2. While in the 18 wt.% solution, the corrosion rate decreased from 2.92 mm/y in deoxygenated solution to 2.40 mm/y in deoxygenated solution. These experiments undoubtedly indicate that the remaining dissolved-oxygen in the solution can increase the corrosion resistance of titanium by accelerating the formation of passive from. After 24 h, the formation of passive film is delayed or even stopped because of depletion of dissolved-oxygen in the solution, hence a decrease in corrosion resistance. According to the literature [23, 36, 38-43], the presence of oxidant will accelerate the formation of passive film on titanium and titanium alloys. These finding also support that the remaining O_2 in the solution can affect the corrosion development of titanium in HCl-acidic fluid.
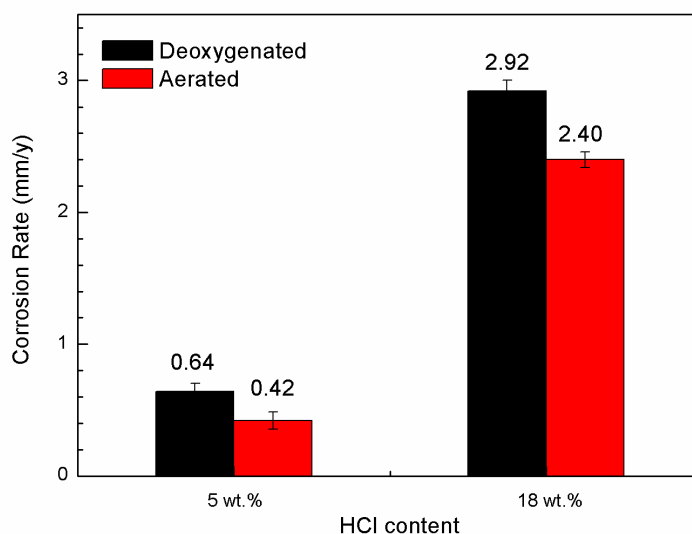
Figure 13. The average corrosion rates of titanium after 72 h of immersion in deoxygenated and aerated 1 wt.% NaCl solution containing different contents of HCl at 40 ^{o}C. The error bars on the figure indicate standard deviation.

5. CONCLUSIONS

In this work, the corrosion behaviors of titanium in HCl-acidizing fluid used in natural gas exploitation were investigated using the polarization curves, electrochemistry impedance spectroscopy and weight loss measurements. The surface morphologies and composition of titanium before and after the immersion in HCl-acidizing fluid were examined using scanning electronic microscope coupled with the energy dispersive spectrometer. It is found that the corrosion rate of titanium in HCl-acidizing fluid strongly depends on the balance between the dissolution and formation of the passive film. The corrosion rate of titanium increases with increasing HCl content. This can be attributed to the dissolution of passive film is enhanced as the HCl content increases. For the long term test, the corrosion resistance of titanium first increases and then decreases with time. The maximum value is present at 24 h. This can be attributed to the remaining dissolved-oxygen accelerates the formation of passive film. As the dissolved-oxygen in solution being depleted, the formation of passive film is delayed or will not be able to form, consequently, there is an continuous decrease in corrosion resistance of titanium in HCl-acidizing fluid after 24 h of immersion.

References

1. R.D. Kane, A. Craig, and A. Venkatesh, Titanium alloys for oil and gas service: A review. NACE Corrosion 2009 Conference & Expo, Atlanta, USA, 2009, Paper No. 09078.
2. M. Gonzalez, K. Maskos, R. Hargrave, J. Kuberry, D. Reeves, J. Grauman, J. Skogsberg and S. Ali, Titanium alloy tubing for HPHT applications. SPE Annual Technical conference and Exhibition, Denver, USA, 2008, SPE 115708.
3. R.R. Boyer, *Mater. Sci. Eng*. A, 213 (1996) 103.
4. A.M. Al-Mayouf, A.A. Al-Swayih, N.A. Al-Mobarak and A.S. Al-Jabab, *Mater. Chem. Phys*., 86 (2004) 320.
5. Y. Bai, Y.L. Hao, S.J. Li, Y.Q. Hao, R. Yang and F. Prima, *Mater. Sci. Eng*. C, 33 (2013) 2159.
6. M.J. Jackson, J. Kopac, M. Balazic, D. Bombac, M. Brojan and F. Kosei, Titanium and titanium alloy applications in medicine, in: W. Ahmed and M.J. Jackson, (Eds.), Surgical tools and medical devices. Springer International Publishing, (2016) Switzerland.
7. A.R. Rafieerad, M.R. Ashra, R. Mahmoodian and A.R. Bushroa, *Mater. Sci. Eng*. C, 57 (2015) 397.
8. U.K. Mudali, R.K. Dayal and J.B. Gnanamoorthy, *J. Mater. Eng. Performance,* 4 (1995) 756.
9. J. Pang and D.J. Blackwood, *Corros. Sci*., 105 (2016) 17.
10. R.W. Schutz and H.B. Watkins, *Mater. Sci. Eng*. A, 243 (1998) 305.
11. Sinopec Corp., Communication on progress for sustainable development, 2015. http://english.sinopec.com/download_center/reports/2015/20160329/download/20160329001en.pdf.
12. B. Chambers, A. Venkatesh and S. Mishael, Performance of tantalum-surface alloy on stainless steel and multiple corrosion resistant alloys in laboratory evaluation of deep well acidizing environments. NACE Corrosion 2011 Conference & Expo, Houston, USA, 2011, Paper No. 11106.

13. D.R. Klink, and R.W. Schutz, Engineering incentives for utilizing Ti-3Al-8V-6Cr-4Zr-4Mo alloy tubulars in highly aggressive deep sour wells. Corrosion 92, 1992, Houston, USA, Paper No. 63.
14. R.D. Kane, S. Srinivasan, B. Craig and K.M. Yap, A comprehensive study of titanium alloys for high pressure (HPHT) wells. NACE Corrosion 2015 Conference & Expo, Dallas, USA, 2015, Paper No. 5512.
15. R.W. Schutz and B.C. Jena, Sour service test qualification of a new high-strength titanium alloy-UNS R55400. NACE Corrosion 2015 Conference & Expo, Dallas, USA, Paper No. 5794.
16. R.W. Schutz, R. Porter and J. Horrigan, Qualification of Ti-6Al-4V-Ru alloy production tubulars for aggressive fluoride-containing mobile bay well service. NACE Corrosion 2000 Conference & Expo, 2000, Orlando, USA; Paper No. 00160.
17. Z.B. Wang, H.X. Hu, Y.G. Zheng, W. Ke and Y.X. Qiao, *Corros. Sci.*, 103 (2016) 50.
18. C. Ciszak, I. Popa, J.M. Brossard, D. Monceau and S. Chevalier, *Corros. Sci.*, 110 (2016) 91.
19. M.D. Pustode, V.S. Raja and N. Paulose, *Corros. Sci.,* 82 (2014) 191.
20. P. Shi, F. Li, Y. Wu, H. Ji, R. Li and X. Wang, *Corros. Sci.*, 93 (2015) 58.
21. H.S. Kim and W.J. Kim, *Corros. Sci.*, 89 (2014) 331.
22. W. Li, B. Brown, D. Young and S. Nesic, *Corrosion,* 70 (2014) 294.
23. L. Wang, X.Q. Cheng, S.J. Gao, X.G. Li and S.W. Zou, *Mater. Corro.,* 66 (2015) 251.
24. X. Wang and H. Xiao, *Int. J. Electrochem. Sci.*, 12 (2017) 268.
25. Y. Xiang, M. Yan, Y. Choi, D. Young and S. Nesic, *Int. J. Greenh. Gas Control,* 30 (2014) 125.
26. D. Zhou, J. Wang, Y. Gao, L. Zhang, *Int. J. Electrochem. Sci.*, 12 (2017) 192.
27. Y. Zheng, J. Ning, B. Brown and S. Nesic, *Corrosion*, 72 (2016) 679.
28. Y. Xiang, Y.S. Choi, Y. Yang and S. Nesic, *Corrosion*, 71 (2015) 30.
29. W. Yan, P. Zhu and J. Deng, *Int. J. Electrochem. Sci.,* 11 (2016) 9542.
30. L.L. Shreir, Electrochemical principles of corrosion: a guide for engineers, Department of Industry, (1982) London, UK.
31. E. McCafferty, Introduction to corrosion science, Springer Science+ Business Media, LLC., (2010) Berlin, Germany.
32. N. Casillas, S. Charlebois, W.H. Smyrl and H.S. White, *J. Electrochem. Soc.*, 141 (1994) 636.
33. S.L. de Assis, S. Wolynec and I. Costa, *Electrochim. Acta,* 51 (2006) 1815.
34. I.C. Lavos-Valereto, S. Wolynec, I. Ramires, A.C. Guastaldi and I. Costa, *J. Mater. Sci. -Mater. Med.*, 15 (2004) 55.
35. M. Pourbaix, Atlas of electrochemical equilibria in aqueous solutions, second ed. National Association of Corrosion Engineers, (1974) Houston, USA.
36. M. Nakagawa, S. Matsuya and K. Udoh, *Dent. Mater.*, 21 (2002) 83.
37. Z.B. Wang, H.X. Hu, C.B. Liu and Y.G. Zheng, *Electrochim. Acta,* 135 (2014) 526.
38. P.R. Shibad and J. Balachandra, *Anti-corros. Methods Mater.,* 23 (1976) 16.
39. I.N. Andijani, S. Ahmad and A.U. Malik, *Desalination,* 129 (2000) 45.
40. A.S. Mogoda, Y.H. Ahmad and W.A. Badawy, *Mater. Corros.,* 55 (2004) 449.
41. J.A. Petit, G. Chatainier and F. Dabosi, *Corros. Sci.,* 21 (1980) 279.
42. T.P. Cheng, J.T. Lee and W.T. Tsai, *Electrochim. Acta,* 36 (1991) 2069.
43. J.R. Cobb and H.H. Uhlig, *J. Electrochem. Soc.,* 99 (1959) 13.